

University of New Hampshire

University of New Hampshire Scholars' Repository

Earth Systems Research Center

Institute for the Study of Earth, Oceans, and
Space (EOS)

3-10-2017

Greenhouse gas balance over thaw-freeze cycles in discontinuous zone permafrost

R. M. Wilson

Florida State University

L. Fitzhugh

Gulf Coast State College

G. J. Whiting

Christopher Newport University

Stephen E. Frolking

University of New Hampshire, Durham, steve.frolking@unh.edu

M. D. Harrison

Christopher Newport University

See next page for additional authors

Follow this and additional works at: <https://scholars.unh.edu/ersc>

Comments

This is an article published by AGU in Journal of Geophysical Research: Biogeosciences in 2017, available online:

<https://dx.doi.org/10.1002/2016JG003600>

Recommended Citation

Wilson RM, L Fitzhugh, G Whiting, S Frolking, MD Harrison, N Dimova, WC Burnett, JP Chanton. 2017. The greenhouse gas balance of organic soils undergoing permafrost thaw, J. Geophys. Res. Biogeosciences, 122, <https://dx.doi.org/10.1002/2016JG003600>

This Article is brought to you for free and open access by the Institute for the Study of Earth, Oceans, and Space (EOS) at University of New Hampshire Scholars' Repository. It has been accepted for inclusion in Earth Systems Research Center by an authorized administrator of University of New Hampshire Scholars' Repository. For more information, please contact Scholarly.Communication@unh.edu.

Authors

R. M. Wilson, L. Fitzhugh, G. J. Whiting, Stephen E. Frolking, M. D. Harrison, N. Dimova, W. C. Burnett, and Jeff P. Chanton

RESEARCH ARTICLE

10.1002/2016JG003600

Key Points:

- Freeze-thaw cycles in discontinuous zone permafrost peatlands result in changing C dynamics over time
- Transient increases in radiative forcing at the initiation of thaw are offset over the lifetime of the peat by net C sequestration
- Integrated over their lifetimes, peatlands are net C sinks with a positive cooling effect on the atmosphere

Supporting Information:

- Supporting Information S1

Correspondence to:

R. M. Wilson,
rmwilson@fsu.edu

Citation:



Wilson, R. M., L. Fitzhugh, G. J. Whiting, S. Frolking, M. D. Harrison, N. Dimova, W. C. Burnett, and J. P. Chanton (2017), Greenhouse gas balance over thaw-freeze cycles in discontinuous zone permafrost, *J. Geophys. Res. Biogeosci.*, 122, doi:10.1002/2016JG003600.

Received 27 AUG 2016

Accepted 30 JAN 2017

Accepted article online 2 FEB 2017

Greenhouse gas balance over thaw-freeze cycles in discontinuous zone permafrost

R. M. Wilson¹ , L. Fitzhugh², G. J. Whiting³, S. Frolking⁴, M. D. Harrison³, N. Dimova⁵, W. C. Burnett¹, and J. P. Chanton¹ 
¹Earth Ocean and Atmospheric Sciences, Florida State University, Tallahassee, Florida, USA, ²Natural Sciences, Gulf Coast State College, Panama City, Florida, USA, ³Organismal and Environmental Biology, Christopher Newport University, Newport News, Virginia, USA, ⁴Earth Systems Research Center, University of New Hampshire, Durham, New Hampshire, USA, ⁵Geological Sciences, University of Alabama, Tuscaloosa, Alabama, USA

Abstract Peat in the discontinuous permafrost zone contains a globally significant reservoir of carbon that has undergone multiple permafrost-thaw cycles since the end of the mid-Holocene (~3700 years before present). Periods of thaw increase C decomposition rates which leads to the release of CO₂ and CH₄ to the atmosphere creating potential climate feedback. To determine the magnitude and direction of such feedback, we measured CO₂ and CH₄ emissions and modeled C accumulation rates and radiative fluxes from measurements of two radioactive tracers with differing lifetimes to describe the C balance of the peatland over multiple permafrost-thaw cycles since the initiation of permafrost at the site. At thaw features, the balance between increased primary production and higher CH₄ emission stimulated by warmer temperatures and wetter conditions favors C sequestration and enhanced peat accumulation. Flux measurements suggest that frozen plateaus may intermittently (order of years to decades) act as CO₂ sources depending on temperature and net ecosystem respiration rates, but modeling results suggest that—despite brief periods of net C loss to the atmosphere at the initiation of thaw—integrated over millennia, these sites have acted as net C sinks via peat accumulation. In greenhouse gas terms, the transition from frozen permafrost to thawed wetland is accompanied by increasing CO₂ uptake that is partially offset by increasing CH₄ emissions. In the short-term (decadal time scale) the net effect of this transition is likely enhanced warming via increased radiative C emissions, while in the long-term (centuries) net C deposition provides a negative feedback to climate warming.

1. Introduction

Permafrost regions at high northern latitudes store an estimated 1300 Pg (±200 Pg) of soil organic carbon (C). Of this quantity, some 500 Pg may seasonally thaw in active layers above the 800 Pg of perennially frozen soil [Hugelius et al., 2014]. Warming air temperature in response to climate change, particularly at high latitudes, may also trigger permafrost thawing [Christensen et al., 2013]. This thawed organic C would then become available for microbial decomposition which ultimately converts soil organic C to the greenhouse gases carbon dioxide (CO₂) and methane (CH₄) [Schädel et al., 2016]. The magnitude of greenhouse gases released from thawing soils differs depending upon a number of factors including, most importantly, changes in soil water content [Blanc-Betes et al., 2016; Natali et al., 2015; Elberling et al., 2013], length of the growing season, warmer winters [Natali et al., 2012], soil temperature [Hicks Pries et al., 2013], active layer depth [O'Donnell et al., 2011], anaerobic conditions, microbial activity, and quantity and composition of the available organic matter [Treat et al., 2014].

Permafrost soils can be broken down into two categories: mineral soils, which generally contain less than 20% C, and peatland soils, which may have 80% or more organic C [Schuur et al., 2015]. In this study, we focused on boreal peatlands in western Canada located in the discontinuous permafrost zone (DPZ) [Tarnocai et al., 2009; Robinson and Moore, 2000]. Here peatlands occupy 365,000 km² in Alberta, Saskatchewan, and Manitoba and store about 48 Pg of C. It is estimated that just over a quarter of these peatlands are underlain by permafrost, representing about 13 Pg of stored C [Vitt et al., 2000a].

Peat plateaus form at this location when ice accretion and expansion during permafrost freezing elevate existing ombrotrophic peat into a raised plateau. This elevation results in drier conditions and colonization by woody vegetation such as black spruce, *Picea mariana* [Vitt et al., 1995]. Within the Canadian DPZ,

shading by the spruce canopy or thermal insulation by *Sphagnum* moss and snow contributes to the persistence of ecosystem-protected permafrost which may be in disequilibrium with mean annual temperature [Halsey et al., 1995; Camill and Clark, 1998; Camill, 1999; Vitt et al., 2000b; Beilman et al., 2001]. Regional warming, as well as disturbance (e.g., fire) to the features and vegetation that have provided shade and insulation, can cause permafrost thawing and a collapse of the plateau. Such collapses often flood resulting in the formation of ~0.5 m deep (relative to the plateau surface) round or oval collapse scar wetlands [Vitt et al., 1995; Camill, 1999; Robinson and Moore, 2000]. Higher productivity coupled with low O₂ conditions in the wetland habitats promote peat accumulation which eventually elevates the collapse scar into a drier bog [Zoltai, 1993]. The ingrowth of *Sphagnum* over the bog sites provides an insulating layer which promotes refreezing thereby starting the cycle all over again [Zoltai, 1993].

Basal fen peat in the region dates back 7000–9000 years [Zoltai, 1993]. Evidence of permafrost is seen as early as 3700 years ago, and these areas have apparently naturally cycled between frozen peat plateau and thawed wetland habitat 2 to 3 times since the end of the mid-Holocene warm period (~3700 years B.P.) [Zoltai, 1993]. In these cycles, canopy disturbance (e.g., fire) is followed by thawing, collapse, and flooding, then *Sphagnum* regrowth, insulation, and refreezing [Zoltai, 1993]. Such cyclical permafrost-thaw cycles are not unique to the Canadian DPZ and have also been reported from permafrost sites in Alaska [e.g., Jones et al., 2013].

Thaw-refreeze cycle time scales vary significantly among sites within the DPZ [Zoltai, 1993]. Some sites may experience complete fire-plateau-fire cycles within 600 years, while other sites experienced no fire activity—and persistence of permafrost plateau—for over 1000 years [Zoltai, 1993]. In Zoltai's [1993] time sequence of peat degradation/aggradation cycles, thaw subsidence following fire occurs rapidly on the order of years, uplift and bog formation follows on the order of decades, and permafrost plateaus may be stable on the order of centuries. Zoltai [1993] examined the stratigraphy of peat cores in sites within the same geographic area as our study and found that sylvic peat, which accumulated on the frozen plateaus, made up only a small portion of the peat at depth; most peat was dominated by *Sphagnum* species which accumulated during the intermittent thaw periods. Given the temporal dominance of permafrost plateaus in Zoltai's [1993] model, the dominance of *Sphagnum* in the cores is striking and likely reflects the resistance of *Sphagnum*-derived organic matter to decomposition [e.g., Hogg et al., 1992], although differential combustion rates of organic materials could also explain the abundance of *Sphagnum* in these cores if *Sphagnum* is less easily combusted than other organic matter present [Turetsky et al., 2004]. Or, the wetter conditions in *Sphagnum*-dominated areas could make bogs less susceptible to fire than the drier plateau stages preferentially preserving *Sphagnum*-derived organic matter in the peat record.

Based upon measurements at similar features, it is believed that the peat plateaus are currently near neutral C balance [Zoltai, 1993; Euskirchen et al., 2014] or serve as weak CO₂ sources [Backstrand et al., 2010] or sinks [Turetsky et al., 2007; Jones et al., 2013, 2016]. Permafrost thawing makes previously frozen C more available to degradation by microbes [Schädel et al., 2016; Schuur et al., 2015; O'Donnell et al., 2012]—which convert peat C to CO₂ and CH₄—leading to concerns about the potential contribution of thawing permafrost to increased C emissions and future climate change. For example, permafrost thawing in the Arctic has mobilized ancient organic C which is rapidly converted to CO₂ via microbial degradation [Schuur et al., 2008; Spencer et al., 2015; Oechel et al., 1993; Zimov et al., 2006; Goulden et al., 1997; Melillo et al., 2002; Eliasson et al., 2005]. However, well-drained peat and mineral soil permafrost sites typically thaw and then drain [Frey and McClelland, 2008; Kawahigashi et al., 2004; Spencer et al., 2015; O'Donnell et al., 2012; Jones et al., 2016] contributing to the expansion of dry habitats. Drying promotes aerobic conditions in the active layer which produce higher CO₂ emissions than anaerobic habitats and stimulates a stronger positive climate feedback upon thaw [Schädel et al., 2016]. In contrast, poorly drained peatland permafrost sites typically thaw and then flood, forming collapse scar wetlands that are dominated by anaerobic conditions [Bellisario et al., 1999]. Poorly drained syngenetic permafrost sites may also experience high C loss rates [e.g., O'Donnell et al., 2012] or decreased C accumulation following thaw [Jones et al., 2013, 2016] as large stores of previously (and rapidly) frozen (i.e., microbially unavailable) labile C become accessible [Schädel et al., 2016]. However, at our site, the bulk of the peat was apparently established under wetland conditions prior to the initiation of permafrost [Zoltai, 1993]. Thus, it had time to accumulate and undergo preliminary degradation before becoming frozen in permafrost. In this case, the labile fraction had likely already been partially consumed prior to freezing possibly lowering subsequent C loss following thaw. Each subsequent thaw cycle would

deplete the labile fraction a bit more, creating the potential for reduced C losses with each successive thaw stage. The low oxygen availability coupled with enhanced primary productivity in the collapse scar wetlands may lead to an increase in the accumulation rate (i.e., enhanced C uptake) at this site—similar to how most of the organic C deposit appears to have originally formed before becoming frozen in permafrost [Zoltai, 1993]. Increased thawing, as a result of current trends in climate at high latitude, could lead to larger thaw features in the DPZ and less chance for the features to refreeze, allowing increased net C storage and, potentially, a negative feedback toward climate change.

As permafrost plateaus transition to wetlands, however, CH₄ emissions also increase [Bellisario *et al.*, 1999] in direct proportion to net ecosystem production (NEP) [Whiting and Chanton, 1993] and temperature [Schädel *et al.*, 2016]. Since the sustained-flux global warming potential (SGWP) of CH₄ is ~45 times that of CO₂ on a 100 year time scale [Neubauer and Megonigal, 2015], there may be a net increase in radiative forcing in the short term following thaw in spite of the increased uptake of CO₂. But, because the lifetime of CH₄ in the atmosphere is much shorter than that of CO₂, the SGWP of CH₄ falls by 67% on the 100–500 year time scale [Neubauer and Megonigal, 2015]. Thus, we hypothesize that over long time scales (centuries to millennia) the influence of CH₄ emissions on the atmosphere will be negligible when the magnitude of CH₄ emissions is small compared to the strength of the CO₂ sink and that the net effect of permafrost to wetland transition on atmospheric greenhouse gas stores will depend on (1) the time scale at which these effects are considered and (2) the proportion of CO₂:CH₄ emitted [Whiting and Chanton, 2001].

To (1) understand C exchange since the formation of these peatlands, to (2) test the hypothesis that peatland permafrost thaw leads to additional C storage, and to (3) evaluate whether the combined CO₂ and CH₄ fluxes of thaw features act as net greenhouse gas (not just C) sources or sinks, we will use three different analytical techniques to describe C exchange over three different time scales. Gas flux measurements will be used to describe instantaneous greenhouse gas exchange at the time of sampling. A radioactive tracer with a relatively short half-life (²¹⁰Pb; $t_{1/2}$ = 22.3 years) will be used to describe net C balance over the last ~150 years. Radiocarbon (¹⁴C; $t_{1/2}$ = 5730 years), which has a much longer half-life, will be used to explore processes going back to the initiation of permafrost, i.e., ~3.7 kya. In the final section we will employ a modeling approach developed by Frohking *et al.* [2006] to evaluate the net radiative forcing due to permafrost-thaw cycles and end with modeling projections for future forcings under different CO₂:CH₄ emission scenarios where permafrost cannot reform due to increased climate warming.

2. Materials and Methods

2.1. Site Description

The town of High Level in Alberta, Canada, is situated on a plateau encircled by hills at approximately 58°N, 117°W. Sampling was conducted at eight sites in the discontinuous permafrost zone north of High Level, Alberta (Figure 1).

Sites HL2, HL3, and HL6 were the northernmost sites located within 100 m of each other, approximately 100 km north of High Level, Alberta. Sites HL7 and HL8 were located within 100 m of each other at approximately 90 km north of High Level. Sites HL1, HL4, and HL5 were the southernmost sites and were located approximately 60 km north of High Level. HL4 and HL5 were within 100 m of each other, while HL1 was located 30 km west of HL4 and HL5.

Each site contained a circular or oblong thaw feature surrounded by permafrost plateau (Figure 2a). The initial stage of the thaw feature is the moat, which is completely inundated. Over time, the ingrowth of *Sphagnum* raises the surface of the feature creating a drier *Sphagnum* lawn which we refer to as the midbog. In between these two features is the bog-moat transition. Between the midbog and the plateau the trailing edge of the thaw feature can refreeze creating a stable edge which transitions into the surrounding permafrost plateau. Vegetational succession was evident progressing from the thaw feature through the permafrost plateau. Water sedge (*Carex aquatilis*), cotton grass (*Eriophorum vaginatum*), bog cranberry (*Oxycoccus microcarpus*), bog rosemary (*Andromeda polifolia*), and leather leaf (*Chamaedaphne calyculata*) were abundant at the fully thawed wetland moat sites. The abundance of sedges and aquatic vegetation decreased near the bog moat transition and bog features. Midbog features contained different species of *Sphagnum* moss, depending on

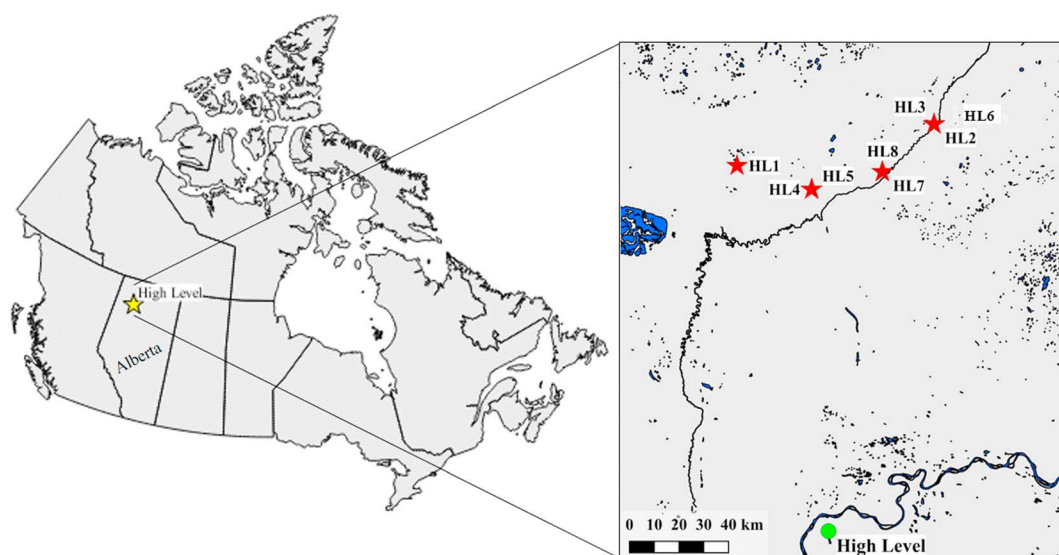


Figure 1. Map of the sampling locations. In the inset the blue lines indicate water bodies, the red stars denote sampling locations, and the town of High Level, Alberta, Canada, is denoted by the green circle. Map created from data obtained from Natural Resources Canada (<http://gdr.aggr.nrcan.gc.ca>).

peat moisture content. Permafrost plateaus were colonized by black spruce (*Picea mariana*), Labrador tea (*Ledum groenlandicum*), lingon berry (*Vaccinium vitis-idaea*), and lichen.

2.2. Gas Flux Measurements

CH₄ and CO₂ flux measurements were collected over 2 years (2001 and 2002) across thaw features at the sites. Flux measurements were conducted by using transparent temperature-controlled phytochambers [Chanton *et al.*, 1992a; Chanton and Whiting, 1995] that were affixed to permanent collars extending 25 cm deep from the peat surface. The phytochambers collected CH₄ and measured CO₂ exchange while maintaining environmental parameters at near ambient conditions. CO₂ concentrations were monitored via a LI-6200 (LICOR Inc., Lincoln, NE, USA), and headspace samples were collected at regularly spaced time intervals for analysis of CH₄ concentrations via flame ionization gas chromatography. To simulate the daily photoperiod, screens of varying density were placed over the chambers and the CO₂ exchange was determined. Respiration was measured by covering the chambers with a blackout cloth. An average of 50 plots (0.43 m² chamber locations) spread across seven sites (HL1, HL2, HL3, HL5, HL6, HL7, and HL8) were sampled every 2 weeks during the growing season (May through September) over a 2 year period. One early (mid-October 2001 when surfaces were starting to freeze) and one midwinter (January 2002) measurements were also taken at each plot to assess emissions under frozen soil conditions. Typically, in early May the sites were still partially frozen; thus, we should have detected any spring flush of gases accumulated during the frozen season had one occurred. We assumed that winter fluxes (November through April) were represented by measurements made in January. From measurements of photosynthetically active radiation daily insolation curves were generated and daily net ecosystem exchange of CO₂ was calculated from the chamber-light-CO₂ response curves. Integrated annual exchanges for each chamber location were calculated by fitting the data with a Gaussian function. Net C flux was calculated by summing the fluxes of CO₂ and CH₄ for each chamber location. Net radiative C fluxes on both 100 year and 500 year time scales were calculated by summing CO₂ flux with the product of CH₄ flux and the global warming potential of CH₄ for the respective time scales [Whiting and Chanton, 2001].

2.3. Core Collection

Peat cores were collected by using an Eijkelpamp peat corer (Eijkelpamp Agrisearch Equipment, Netherlands) from the same sites at which flux measurements were taken. Most cores were collected from the middle of the thaw features (midbog following the designations in Figure 2). At selected sites an additional core was also collected at the bog-moat transition; the moat, stable edge, and one core were collected from the permafrost plateau at site HL2. The surface peat (0 to 20 cm deep) was sampled with a bread knife. The

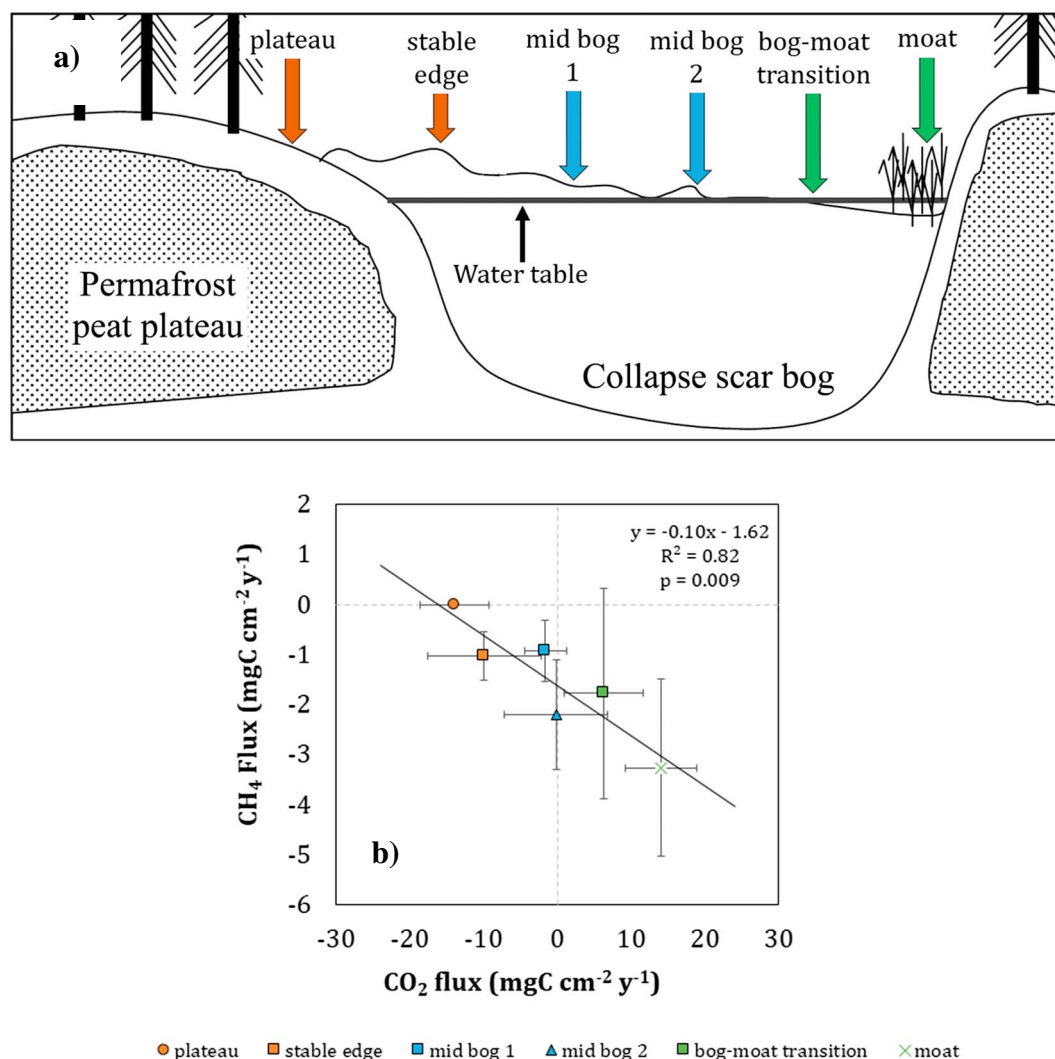


Figure 2. (a and b) CH₄ and CO₂ flux across thaw features including noncored sites. Negative fluxes indicate loss to the atmosphere; positive CO₂ fluxes indicate C uptake by the ecosystem. In Figure 2a, the colored arrows indicate the different habitat types and correspond with the color of points in the bottom panel (adapted from Prater *et al.* [2007]). In Figure 2b, symbols represent average values and the uncertainty bars represent the standard deviation of values from each habitat type. The dashed lines indicate zero flux. The solid line represents the results of the linear regression.

frozen permafrost plateau core was collected to 246 cm by using a concrete hole saw on a rotary drill. After collection, the cores were frozen and sliced into 3 cm sections, freeze-dried and ground to a homogenous powder.

2.4. Physical Characteristics of the Peat

The change in sample mass during freeze drying was used to estimate the percent water content of the peat. The dry bulk density (B_D) of the peat was determined by calculating the volume change upon adding a known mass of the unground dry peat to 5 mL of water. The porosity (P_s) of the sample was determined from the grain density (ρ), which we assumed to be 1.0 for organic matter, and the bulk density (B_D) of the peat by equation (1):

$$\varphi = (\rho_s - B_D) / \rho_s \quad (1)$$

2.5. Radionuclide Analyses

Each 3 cm core section from the peat surface to the deepest depth of detectable ²¹⁰Pb activity (up to ~1 m deep) was analyzed separately. Lead-210 (²¹⁰Pb) activity was analyzed by alpha spectrometry by using the

activity ratio of the shorter-lived granddaughter polonium isotope ^{210}Po ($t_{1/2} = 138$ days which is assumed to be in secular equilibrium with the parent ^{210}Pb) to an internal tracer, ^{209}Po ($t_{1/2} = 125$ years). A known activity of ^{209}Po was added to each sample then the $^{209}/^{210}\text{Po}$ was leached from the peat by refluxing for 4 h with concentrated nitric acid. The Po isotopes were then coprecipitated with FeOH from the resulting nitric acid solution by addition of concentrated ammonium hydroxide. The resulting precipitate was collected and redissolved in dilute hydrochloric acid and the pH adjusted to 2. A silver disk, with one side covered in plastic tape, was placed into the FeOH-HCl solution then hydroxylamine hydrochloride, sodium citrate, and ascorbic acid were added to prevent interferences from Fe and other metals. The silver disk was exposed to the resulting solution at 90°C for 3 h. The silver disk was removed from the solution, rinsed with distilled water, and dried before counting via alpha spectrometry. Additionally, dry peat samples were ground, packed in vials, and counted on a well-type germanium gamma detector to evaluate activities of the supported ^{226}Ra ($t_{1/2} = 1600$ years) via the ^{214}Pb and ^{214}Bi photopeaks at 295 keV, 352 keV, and 609 keV. Since there was no ^{226}Ra detected in these mineral-free peat samples, all of the ^{210}Pb is assumed to come from atmospheric deposition and not from the radioactive decay of ^{226}Ra ; i.e., all of the ^{210}Pb is "excess."

2.6. ^{210}Pb Dating Model

Peat ages for each core section were calculated from the ^{210}Pb activities by using the constant-rate-of-supply model (CRS) [Appleby and Oldfield, 1978, 1983; Appleby, 1993]. The CRS model was chosen over the constant initial composition model because there was a subsurface maximum in ^{210}Pb activity in most of the cores, suggesting that the peat accumulation rate has not been constant over time. In the CRS model, the inputs of ^{210}Pb and peat are independent, and variations of peat accumulation will not affect the cumulative ^{210}Pb inventory. The CRS model calculates age from variation in the ^{210}Pb inventory as a function of depth, assuming a steady state flux (constant rate of supply) of ^{210}Pb over time. In the CRS model, the age (τ) at depth (X) is calculated from the decay constant ($\lambda = 0.0311 \text{ year}^{-1}$ for ^{210}Pb), the total inventory of excess ^{210}Pb at the site (I_T), and the inventory of excess ^{210}Pb below the depth of interest (I_X) by equation (2):

$$\tau = \frac{1}{\lambda} \cdot \ln\left(\frac{I_T}{I_X}\right) \quad (2)$$

An apparent C accumulation rate (aCar) was calculated by multiplying the bulk density of each core section by the section thickness (3 cm) and summing those results from the surface to the depth at which no ^{210}Pb activity was detectable in each core and dividing by the peat age at that depth. These estimates were then multiplied by 0.45, assuming that the peat was approximately 45% C by dry weight (based on our findings at other peatlands [e.g., Tfaily et al., 2014]) to yield an aCar in terms of $\text{mg C cm}^{-2} \text{ yr}^{-1}$. The average across all sites for the three main habitat types: permafrost, midbog, and moat, are reported in Table 1.

2.7. Radiocarbon (^{14}C) Dating of Selected Cores

Radiocarbon analysis on 8 sections of the permafrost core (from 50 cm to 246 cm deep) and 2–3 sections of HL1, HL2, and HL8 was conducted by bomb combustion of peat followed by cryogenic purification of resultant CO_2 that was stripped from vials with He. These methods are described in more detail in Corbett et al. [2013]. ^{14}C analyses were performed at the National Ocean Sciences Accelerator Mass Spectrometry facility, Woods Hole Oceanographic Institute (Woods Hole, MA). Radiocarbon-based C accumulation rates were calculated by dividing the cumulative bulk density (i.e., the sum of the bulk densities of each section multiplied by their respective thickness) of the core by the ^{14}C -age of the deepest section, then multiplying by 0.45 (assuming peat was 45% C as above). The results for the single permafrost core and the average of the two analyzed midbog and bog-moat transition cores (from HL2 and HL8) are reported in Table 1.

2.8. Modeling Radiative Forcing

We used the radiative forcing model of Frolking et al. [2006], which simulates net greenhouse gas emission impacts on atmospheric radiative forcing as an impulse-response process [e.g., Joos et al., 2013], to calculate net radiative forcing (RF) of these features by taking into consideration the higher sustained-flux global warming potential of CH_4 and the C sequestration of the peat since initial permafrost formation at the end of the mid-Holocene (when the freeze-thaw cycles initiated). In this model, the rest of the Earth system is considered an infinite CO_2 reservoir for the time scales under consideration, with which atmospheric CO_2 pools with residence times much less than the total age of the peatland can equilibrate following a first-order

Table 1. CH₄ and CO₂ Chamber Flux Measurements, ²¹⁰Pb-Based Apparent Accumulation Rates (aCar), and ¹⁴C-Based Apparent Accumulation Rates (aCar) at Sites Where Cores Were Collected

Site	CH ₄ Flux (kg C m ⁻² yr ⁻¹)	CO ₂ Flux (kg C m ⁻² yr ⁻¹)	Net C Balance ^d (kg C m ⁻² yr ⁻¹)	²¹⁰ Pb-aCar ^e (kg C m ⁻² yr ⁻¹)	¹⁴ C-aCar ^e (kg C m ⁻² yr ⁻¹)
Moat	-0.03 ^a ± 0.02	+0.14 ± 0.05	+0.11 ± 0.10	0.80 ± 0.50	na
Bog-moat transition	-0.02 ± 0.02	+0.06 ± 0.05	+0.04 ± 0.10	0.78 ± 1.4	0.01 ± 0.001
Midbog	-0.01 ± 0.01	-0.02 ± 0.03	-0.03 ± 0.03	0.40 ± 0.30	0.01 ± 0.001
Permafrost plateau	BDL ^b	-0.14 ± 0.00	-0.14 ± 0.05	0.20 ± 0.03	0.01 ± na ^c

^aPositive flux numbers indicate net uptake by the system; negative numbers indicate loss to the atmosphere.

^bCH₄ flux from permafrost was below the detection limit (BDL).

^cOnly one permafrost core was collected.

^dNet carbon balance = NCB.

^e²¹⁰Pb-aCar are calculated over the last 100 years, while ¹⁴C-aCar are calculated over the last 2500–3000 years.

equilibration process [Frolking *et al.*, 2006]. The inventory of the long residence time atmospheric CO₂ pool (modeled here as 10⁸ years) does not equilibrate significantly on the order of peatland lifetime (10³–10⁴ years), thus C losses from that reservoir are considered permanent for our purposes (i.e., sequestration as peat [Frolking *et al.*, 2006]).

We modeled freeze-thaw cycles as permafrost plateau followed by moat formation followed by midbog and then back to permafrost. Based on Zoltai [1993], we modeled two different scenarios: a short-frequency freeze-thaw cycle of 600 year duration repeating from the initiation of permafrost (3700 years B.P.) to the present and a long-frequency freeze-thaw cycle of 1000 years repeating from the initiation of permafrost to the present. The duration of each stage within a cycle was derived from Zoltai's [1993] characterizations which gave 10 years for moat habitat, 100 years for bog accumulation, and the remainder of the cycle (490 years for the short cycle and 890 years for the long cycle) for the plateau stage. In short, this gave six 600 year cycles repeating from the end of the mid-Holocene (3700 years B.P.) to the present for the short-frequency scenario, and the long-frequency scenario had approximately four 1000 year cycles repeating from the end of the mid-Holocene to the present. Model parameters for CH₄ emissions from each habitat type were the average measured values from the flux chambers in kg C m⁻² yr⁻¹. For CO₂ uptake we used the average ²¹⁰Pb-derived peat accumulation rates for each habitat type converted to kg CO₂ m⁻² yr⁻¹, by assuming that the peat had an average C content of 45% [e.g., Tfaily *et al.*, 2013]. The results of the model were in net radiative forcing (W m⁻²) of the greenhouse gas balance of the peat since the initiation of permafrost based on each of these two scenarios.

In a second modeling exercise, we projected what would happen if future climate warming interrupted the freeze-thaw cycles by preventing the system from reforming permafrost. In that scenario, we modeled the long-frequency freeze-thaw cycles starting at the initiation of permafrost (3700 years B.P.) repeating until the present and then forced the system to remain a midbog from the current year projecting forward ~400 years. We repeated this exercise incorporating different CO₂ uptake to CH₄ emission scenarios including the current midbog flux ratio value of CO₂:CH₄=40 (on a mol per mol basis), and simulations of ratios=20, 10, 5, and 2 to predict what effect CO₂:CH₄ ratios have on the RF response to permafrost interruption.

3. Results

3.1. Instantaneous C Exchange: Results From Gas Flux Measurements

Across the thaw features, net ecosystem CO₂ exchange switched from net CO₂ emission (negative values by our sign convention) at the plateaus to net CO₂ uptake (positive values by our sign convention) in the moats (Figure 2). Conversely, CH₄ emissions were lowest in the plateaus and increased with thaw stage, with the highest CH₄ emissions observed in the moats (Figure 2). There was a significant correlation between CO₂ and CH₄ fluxes ($R^2 = 0.85$, p -value = 0.009) where higher CH₄ emitting sites also had higher CO₂ uptake.

Summing the annual fluxes of CO₂ and CH₄ allowed us to calculate the net C exchange with the atmosphere at each feature. The annual net C balance (NCB), which is the difference between net ecosystem production

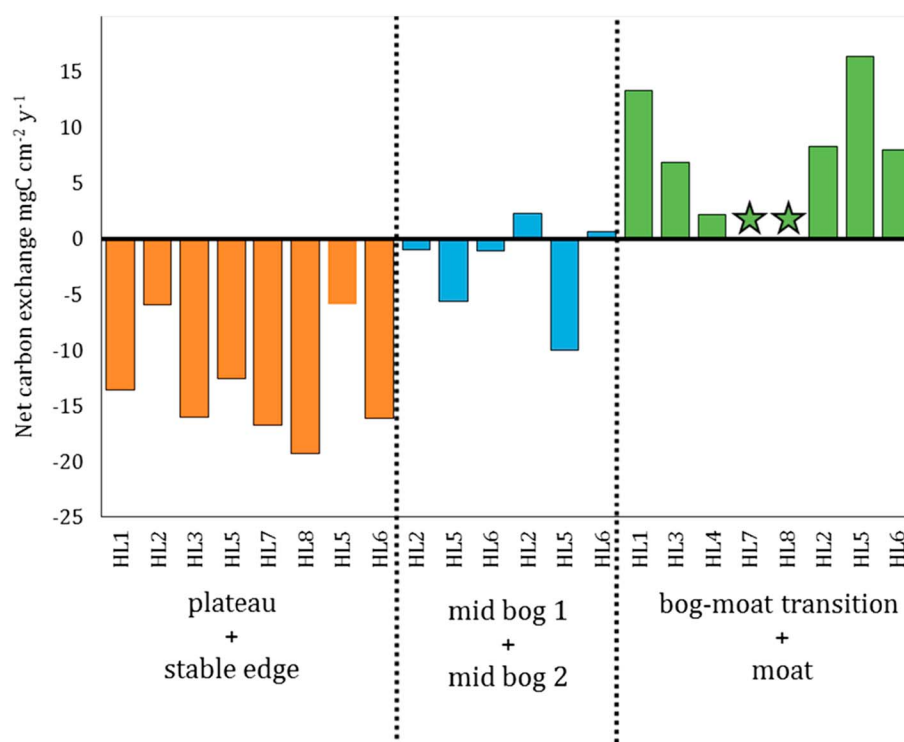


Figure 3. Net C exchange with the atmosphere from the sum of CH₄ and CO₂ fluxes derived from chamber measurements (including noncored sites). Positive numbers indicate C uptake by the ecosystem; negative numbers indicate C lost to the atmosphere. The stars indicate near zero (though still positive) values that were difficult to discern on this scale.

and C loss from the system (as CO₂, CH₄, or dissolved organic carbon (DOC)) in a given year [Frolking *et al.*, 2014], is calculated as the difference between CO₂ uptake and CH₄ emissions (ignoring DOC losses). In this study, a negative net C flux indicates that C is being lost to the atmosphere and the feature is therefore acting as a net C source with a net warming effect. Positive net C fluxes indicate that C is being taken up by the ecosystem and the feature is therefore acting as a net C sink, presumably incorporating C into vegetation biomass, ultimately resulting in peat accumulation and a net cooling effect. Net C exchange indicated that all plateaus and stable edge features were sites of net C loss to the atmosphere (Figure 3). Midbog habitats exhibited mixed results where some sites were characterized by net C loss and some sites were characterized by net C uptake. All bog-moat transition and moat sites were sites of net C uptake, although two of the sites (HL7 and HL8) had very low C uptake rates. CH₄ emissions at these two sites were similar to other moat sites (0.9–1.4 mg C cm⁻² yr⁻¹); thus, the low net C uptake seems to be due to low ecosystem productivity at the site where CO₂ uptake rates are low (1.03–1.5 mg C cm⁻² yr⁻¹; Figure 3).

3.2. Past 150–3400 Year C Exchange: ²¹⁰Pb and ¹⁴C Results

The permafrost site had the steepest decline in ²¹⁰Pb activity with depth (Figure 4) indicating low peat accumulation rates. Sites HL1, HL6, HL7, and HL8 all had an obvious subsurface maximum in ²¹⁰Pb activity, suggesting a recent increase in peat accumulation rates either due to an increase in net ecosystem production (NEP) at these sites or a decrease in surface C losses. Below this subsurface maximum and at all other sites (except HL4), there was a steady decline in ²¹⁰Pb activity with depth consistent with radioactive decay and a constant rate of supply of ²¹⁰Pb. There was no evidence of large C losses such as we would expect from fire, suggesting that the last fire at our study sites was more than 100 years ago. When plotted against cumulative mass depth (Figure S1 in the supporting information) all sites, including HL4, showed a general decline in ²¹⁰Pb activity with depth consistent with decay, indicating that there was variability in peat density or accumulation rates in the HL4 site that obscured the depth trends. The subsurface maximum was still present at HL1, HL6, HL7, and HL8 when viewed in this way.

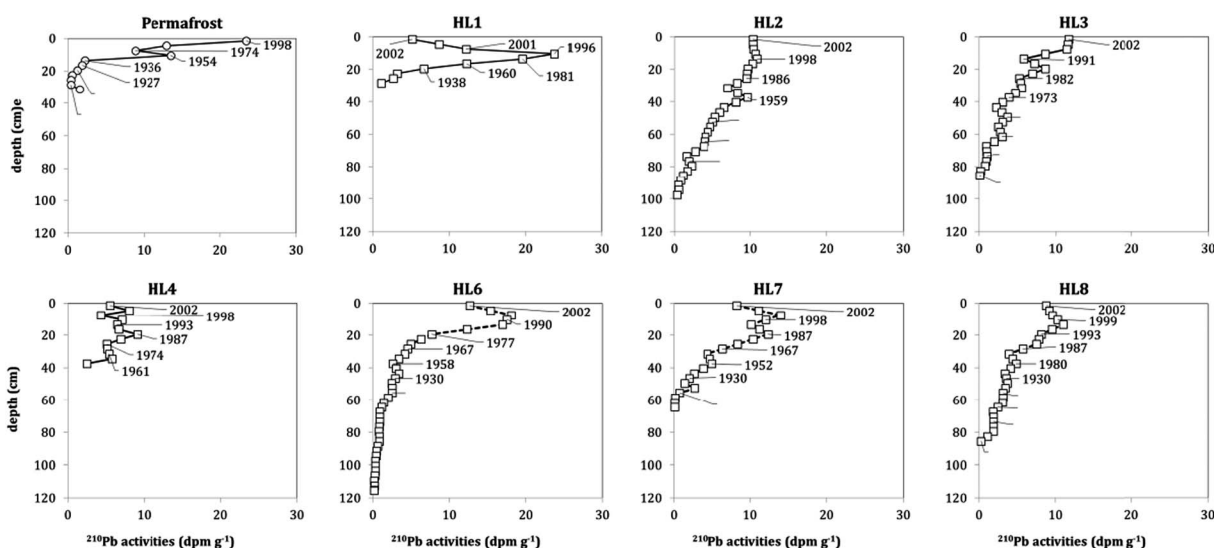


Figure 4. ^{210}Pb activity (dpm g^{-1}) depth profiles. The first panel represents the results from the permafrost plateau core. Each subsequent panel represents the results from the middle of one of the thaw features (midbog 1 following the designations in Figure 1). Dates are based on ^{210}Pb activities using the CRS-model (see text).

The apparent C accumulation rate (aCar) was calculated from the cumulative mass to the deepest dateable horizon (in g m^{-2}) divided by the maximum age of the ^{210}Pb . This ^{210}Pb -based aCar was much higher than NCB estimates at all sites (Table 1).

When radiocarbon (^{14}C) values were plotted against depth, there was a monotonic decrease with cumulative mass depth across all sites which we interpret as an increase in peat age (Figure 5). Permafrost plateau radiocarbon depth profiles were consistent with results from the thaw features. We calculated ^{14}C -based aCar over the entire depth sampled for each of five cores (HL2 bog, HL2 bog-moat transition, HL8 bog, HL8 bog-moat transition, and HL2 permafrost) analyzed for radiocarbon. The results for the single permafrost core and the average of the two bog and bog-moat transition cores are reported in Table 1. All sites had a ^{14}C -based apparent accumulation rate of $0.01 \pm 0.001 \text{ kg C m}^{-2}$ (Table 1). This indicates that over the last 3000 years the sites have accumulated approximately 30 kg C m^{-2} .

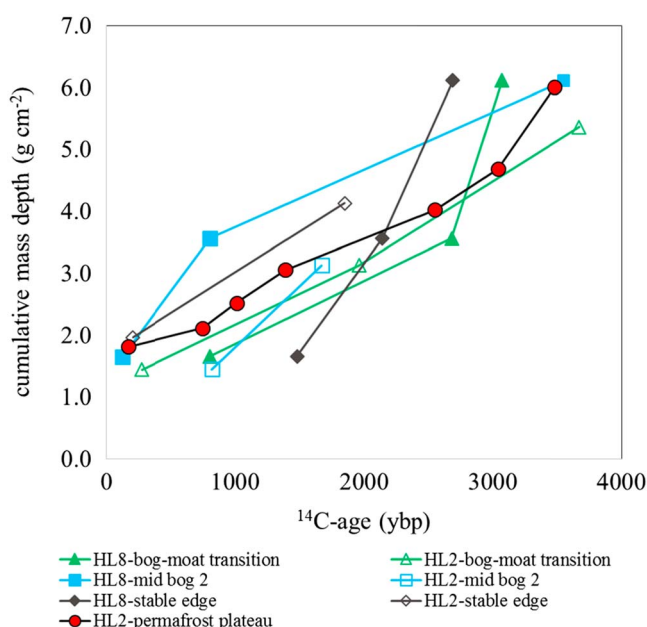


Figure 5. Radiocarbon results. Results are plotted versus cumulative mass depth calculated as described in the text.

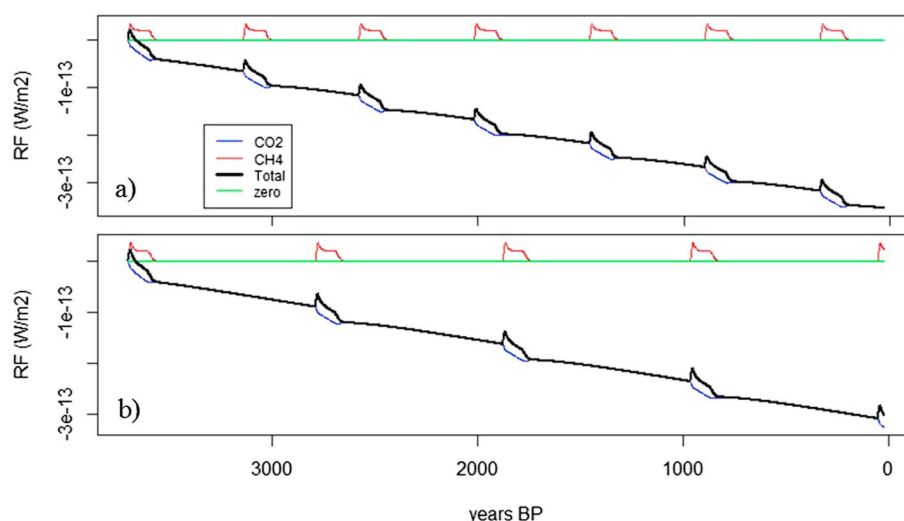


Figure 6. Modeling results of radiative forcing impact per square meter of peatland area. (a) 600 year freeze-thaw cycle. (b) 1000 year freeze-thaw cycle. The green line tracks 0 radiative forcing (RF), i.e., the break-even point. The red line represents the contribution from CH_4 emission. The blue line represents the contribution from CO_2 uptake. The black lines represent the total radiative forcing of the peatland accounting for both CO_2 uptake and CH_4 emission. A negative RF represents a net overall cooling effect. The net RF is relative to the system at peat initiation 3700 years B.P..

3.3. Radiative C Flux: Net Greenhouse Gas Effect

We used the modeling approach of *Frolking et al.* [2006] to calculate the net radiative forcing over the lifetime of the peat under several different scenarios. In the first two scenarios, we allowed the simulation to cycle between permafrost plateau and thaw feature on either 600 year cycles or 1000 year cycles going back to initiation of permafrost thaw 3700 years ago (as per *Zoltai* [1993]) (Figure 6). In both short- and long-frequency thaw cycle models radiative forcing (RF) increased at the initiation of thaw. However, because the moat stage, where RF trends toward net warming, is short-lived relative to the bog and plateau stages, the positive RF effect is correspondingly short-lived. Transition of the system to the bog stage, where the ratio of CO_2 uptake to CH_4 emission is higher, resulted in a decline in the total RF of the system. Permafrost, the longest-lived stage of the cycle, has zero CH_4 emissions, and resulted in a declining RF for the system due to slow CO_2 uptake and sequestration in peat. This long-term stage drove the results for the overall system, so despite the slow sequestration during this stage, when these oscillating landforms are considered across millennia, net cooling results.

In another series of simulations, we modeled the RF of the system if permafrost never reformed at the site following the last thaw cycle, but rather the system transitioned from moat to bog and thereafter remained a bog indefinitely. We also investigated the effect of changing the CO_2 uptake to CH_4 emission rates in the final bog stage to understand the effect of this ratio on the total RF of the system (Figure S2). In a progression of simulations ($\text{CO}_2:\text{CH}_4 = 40, 20, 10, 5$, and 2 mol:mol), RF declined at a successively faster rate in the final bog stage. This resulted because the bog has a stronger net negative effect on RF than the permafrost plateau stage which dominated earlier cycles. Only in the final case where CH_4 emissions were allowed to equal $\frac{1}{2}$ of CO_2 uptake rates did the net RF ever trend positive. In all other scenarios, the net RF in the final stage remained negative in spite of the persistence of the thaw stage. But even in this most extreme case where CO_2 uptake to CH_4 emission ratio was equal to 2, the positive RF stage was transient, lasting approximately 500 years before the system achieved a net negative (cooling) RF again.

In the final series of simulations we modeled the long-frequency freeze-thaw scenario again, this time solving for the amount of C that would need to be emitted from the moat feature to result in a modeled C inventory that matches the measured ^{14}C -based moat inventory. Based on our work at other collapse features, we constrained the $\text{CO}_2:\text{CH}_4$ flux ratios to be equal to 10 [*Hodgkins et al.*, 2015]. The model required CO_2 net emission fluxes of $12.5 \text{ kg CO}_2 \text{ m}^{-2} \text{ yr}^{-1}$ for 10 years—and CH_4 emissions of 1.25 kg m^{-2} —at the initiation of each thawing event in the long-frequency freeze-thaw scenario to yield a total C inventory matching the ^{14}C -based rate of approximately $30 \text{ kg peat C m}^{-2}$ (Figure 7a).

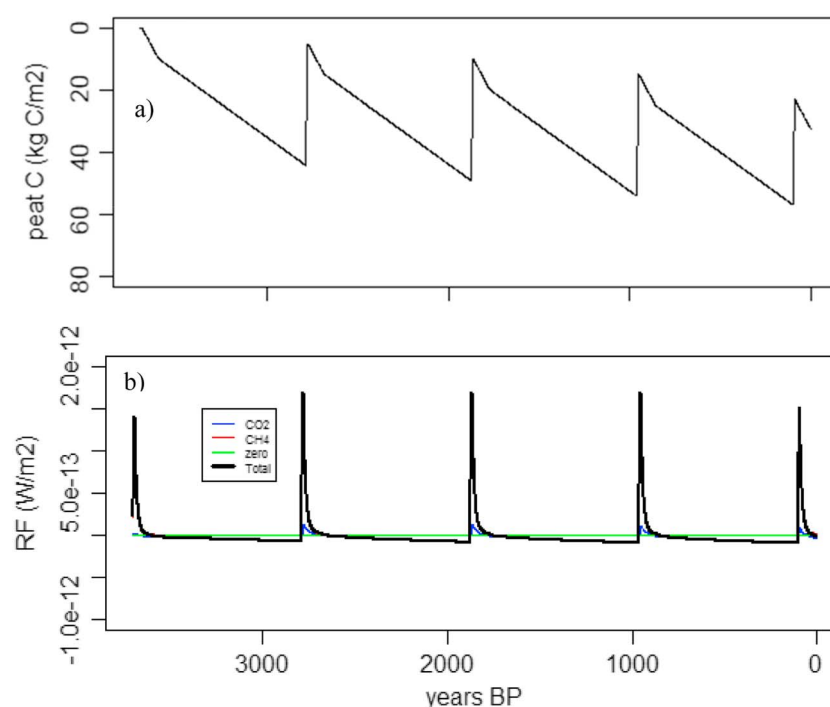


Figure 7. (a) Peat C inventory based on a long-frequency freeze-thaw cycle (1000 years) with CO₂ emissions of 12.5 kg CO₂ m⁻² yr⁻¹ and methane emissions of 1.25 kg CH₄ m⁻² yr⁻¹ which occur for the immediate 10 years after each thaw, consistent with large decomposition events accompanying permafrost thaw. These fluxes result in a peat C inventory of ~30 kg C peat m⁻² which matches the ¹⁴C-based apparent accumulation rate. (b) Net radiative forcing results based on these model inputs. As in the previous figure: The green line tracks 0 radiative forcing (RF), i.e., the break-even point. The red line represents the contribution from CH₄ emission. The blue line represents the contribution from CO₂ uptake. The black lines represent the total radiative forcing of the peatland accounting for both CO₂ uptake and CH₄ emission. A negative RF represents a net overall cooling effect. The net RF is relative to the system at peat initiation 3700 years B.P.

4. Discussion

4.1. Instantaneous C Exchange: Results From Gas Flux Measurements

Net ecosystem exchange of CO₂ and CH₄ emissions were inversely correlated across thaw features in the Canadian DPZ (Figure 2). As observed at some [e.g., Backstrand *et al.*, 2010], though not all [e.g., Euskirchen *et al.*, 2014] other sites, the surface of the permafrost plateaus in our study were sites of net CO₂ emission (negative CO₂ flux values), while CH₄ emissions from the plateaus were negligible during the study period (2001–2002). CH₄ emissions were greatest at the moats and bog-moat transitions where aquatic macrophytes such as *Carex* and *Eriophorum* (spp.) dominate. The high primary productivity of sedge species in marshy thaw and thaw edge features creates CO₂ demand, while the flooded conditions limit oxygen diffusion and facilitate anaerobic CH₄ production. Further, well-developed aerenchyma in marsh plants can facilitate CH₄ fluxes to the atmosphere by providing direct conduits that bypass aerobic peat layers where the CH₄ might otherwise be oxidized [Chanton *et al.*, 1992b]. The inverse correlation between net ecosystem CO₂ exchange and CH₄ emissions supports and extends earlier work showing that as peatland permafrost thaws and transitions to wetland, CO₂ uptake increases, resulting in the wettest sites becoming net CO₂ sinks, with a concomitant increase in CH₄ emissions along that same gradient [Prater *et al.*, 2007; Bellisario *et al.*, 1999].

Across thaw features, we saw a distinct shift from plateaus and stable edges—which flux measurements suggest were net atmospheric C sources—to the moats which were net C sinks at all sites (Figure 3). However, the flux chambers exclude trees greater than 1 m tall which are likely a nontrivial source of CO₂ uptake on the plateaus. Because the chambers do potentially include both root respiration and aboveground and belowground tree-derived litter and the resultant decomposition, but not aboveground tree respiration nor tree photosynthesis, the instantaneous flux measurements may be overestimating net CO₂ emissions at treed sites (i.e., the plateaus). Thus, our results may be underestimating the C sink potential of the plateaus. This finding is consistent with evidence from the ²¹⁰Pb analyses, which show overall accumulation in the

plateau. Additionally, instantaneous flux measurements can vary substantially on a time scale of years and may not reflect long-term trends. For example, permafrost plateaus in Alaska switch between net CO₂ emission and net CO₂ uptake from year to year apparently based on stimulation of ecosystem respiration rates triggered by warmer than mean growing season temperatures or deviation from mean precipitation rates [Euskirchen *et al.*, 2014].

Contrary to the implications of net C estimates at this Alberta site—which indicate net C accumulation following thaw—recent thaw has led to declines in organic C storage at an Alaskan permafrost peatland [O'Donnell *et al.*, 2012]. The Alaskan system of syngenetically formed permafrost, where organic material accretes at the base of the active layer, fundamentally differs from that found in the Alberta DPZ. Unlike the Alaskan permafrost peatland which has been frozen essentially since formation, the Alberta peatland under current consideration has undergone many freeze-thaw cycles over the last 3700 years [Zoltai, 1993]. We posit that at the Alaska site, permafrost formation at the base of the active layer slows or halts decomposition of the available fraction of labile organic matter present, effectively preserving it until such time as the permafrost thaws. In contrast, the DPZ Alberta site has undergone several permafrost-thaw cycles and decomposition of the labile organic matter fraction has been sustained at cumulatively higher rates over time. We expect that each thaw cycle may initiate some transitory increase in decomposition of the thawed organic matter but that the increase in decomposition following each new permafrost-thaw cycle will be less and less until the labile fraction of organic matter is largely depleted. At our site, which has undergone many such permafrost-thaw cycles, the C balance data would suggest that the available labile organic C now supports less decomposition than the concomitant increase in primary production induced by warmer temperatures and thaw. In this sense, we could expect that the response of these sites to increased climate warming may be more similar to nonpermafrost boreal peat deposits which experience limited C loss with warming [e.g., Wilson *et al.*, 2016] than to syngenetic permafrost peatlands which experience large C losses in response to elevated temperatures [e.g., O'Donnell *et al.*, 2012].

4.2. Past 150–3400 Year C Exchange: ²¹⁰Pb and ¹⁴C Results

In general, ²¹⁰Pb activity in our cores decreased with depth (Figure 4), consistent with expectations from radioactive decay. Some sites exhibited a shallow subsurface maximum in activity that could not be attributed to changes in the density of the peat (as evidenced by the persistence of the subsurface maximum when activities were plotted against mass depth (Figure S1) but was probably the result of changes in peat accumulation rates due to decadal-scale variability in primary productivity. It would appear that a recent increase in productivity followed the ²¹⁰Pb maxima at several of our sites, diluting the ²¹⁰Pb arriving from atmospheric deposition and resulting in an increase in activity below the peat surface. In general, these slight deviations will not influence our conclusions as the overall trend was for ²¹⁰Pb activity to decrease with depth, and we calculate ages from the change in the ²¹⁰Pb inventory as a function of depth, assuming that peat growth and ²¹⁰Pb inputs are independent parameters.

The gas flux results (NCB, previous section) provide a snapshot of instantaneous C exchange at these sites as it was occurring during the measurement year. If net CO₂ uptake exceeds CH₄ emissions (i.e., NCB is positive) over a long enough time period, peat accumulates. A peat core, on the other hand, records the sum of C litter inputs and subsequent C losses through degradation across decades to millennia allowing us to infer time-integrated C dynamics. Net peat accumulation at the site since the flux measurements were conducted [D. Olefeldt, *personal communication*, 2015] suggests that these instantaneous flux measures may not provide the full picture of how the peatland is responding to thaw over time. The ²¹⁰Pb measurements extend our view to help us understand C source/sink dynamics at these sites integrated over the recent past (~150 years).

The observed difference between instantaneous NCB and ²¹⁰Pb-based aCar can be explained by understanding the differences between these two measures. NCB and aCar over any specific time period are not directly comparable, in part, because aCar integrates over a much longer time period than NCB and, in part, because the NCB at any time is influenced by the degradation of all older underlying peat layers through the C loss term [Frolking *et al.*, 2014]. By virtue of how it is defined, aCar must always be positive, while NCB for any time point can be either positive or negative. NCB depends on decomposition occurring at the time period being evaluated but is independent of decomposition occurring after that date, while aCar is influenced by decomposition occurring from deposition up to the moment of sampling [Frolking *et al.*, 2014]. Cumulatively, these

differences dictate that when integrated over the entire peat profile, NCB and aCar must be equal, although they may be quite different for any given subset of the peat record.

Although ^{210}Pb measurements indicate that surface (shallowest 100 cm) peat accumulation rates exceed C loss on the decadal scale (Table 1)—and indeed the subsurface maximum in ^{210}Pb activity is consistent with a recent increase in peat accumulation rate—C loss from deep soils (below the depth where ^{210}Pb was detectable) could be exceeding surface accumulation rates leading to net C losses from the ecosystem despite positive accumulation rates at the surface [Hicks Pries *et al.*, 2011]. One way to evaluate deep soil losses is through the use of a longer-lived radioisotope tracer. Radiocarbon (^{14}C) has a half-life of ~5730 years and can therefore be used to understand processes occurring since the formation of the peat deposit.

The ^{14}C -based aCar is lower than the ^{210}Pb -based aCar by an order of magnitude (Table 1). The disparity in calculated accumulation rates between these two geochronological tracers is well described and known as the “Sadler effect” [Sadler, 1981]. The short-term tracer (^{210}Pb) generally reflects only accretion, whereas the longer-lived tracer integrates periods of nondeposition and even net losses which decrease the apparent accumulation rate. We expected the ^{14}C -based aCar to be lower than ^{210}Pb -based aCar for four reasons. First, we expect that some net C loss may have occurred (as net CO_2 emission), while the area was frozen as permafrost. However, the exclusion of trees from the chamber measurements makes this possibility equivocal as permafrost plateaus may be sites of net C accumulation if tree uptake is considered. This possibility is consistent with ^{210}Pb data, which suggest net peat accumulation during plateau stages. Second, the ^{210}Pb rates from currently thawed areas can be assumed to represent above average rates of C accumulation at a given location. This is because ^{14}C integrates over longer time periods encompassing many freeze-thaw cycles during the majority of which time the peat was likely frozen and accumulation rates were much lower than in the currently thawed conditions [Zoltai, 1993; Turetsky *et al.*, 2007]. Conversely, ^{210}Pb -based measurements encompass only a very small fraction of the freeze-thaw cycle, and in sites that are currently thawed the ^{210}Pb -aCar will be dominated by the higher accumulating thaw conditions. The third reason ^{210}Pb aCar were expected to be higher than ^{14}C -aCar is because it is probable that higher atmospheric CO_2 levels and enhanced atmospheric N-deposition have increased primary productivity in the recent past leading to faster peat accumulation rates since the most recent permafrost thaw [Eisenhauer *et al.*, 2012]. This may also explain the apparent increase in peat accumulation diluting the ^{210}Pb in the surface of several of the profiles (Figure 4). The fourth possible reason we may expect is that a mismatch between ^{210}Pb accumulation rates and ^{14}C -based measures is large C loss due to fires initiating the thaw events. Fires in northern boreal peatlands—particularly across the drier plateau features—are capable of burning up to two thirds of the top 20 cm of peat in a single fire event resulting in the rapid conversion of peat C to atmospheric CO_2 [Turetsky *et al.*, 2002; Zoltai *et al.*, 1998]. Again, the long integration time of the ^{14}C -aCar compared to the ^{210}Pb -aCar means that any such catastrophic losses of C are incorporated into the ^{14}C record—resulting in lower apparent C accumulation rates—that may not be captured by the ^{210}Pb record.

We might expect past permafrost stages to result in temporarily slower ^{14}C -based accumulation rates and interruptions in C accumulation due to fire losses to introduce variability into the long-term ^{14}C -aCar trend for this region. Nevertheless, the trend in ^{14}C content from the surface to deep in all examined cores indicates relatively constant accumulation throughout the last 3–4 kya, at least at the resolution sampled (Figure 5).

The apparent constancy of the ^{14}C -based accumulation trend suggests that the site has acted as a net C sink since peat began to form—except for episodic losses due to fire which the ^{14}C record may not have the resolution necessary to reflect—despite evidence of repeated permafrost-thaw cycles. The ^{14}C ages from the frozen permafrost plateau agree well with the ages across all of the thaw features (Figure 5). The inference from these findings is that the surface at these sites cycles between plateau and wetland such that rates of C accumulation are fairly constant from location to location over time; i.e., any periods of rapid C loss following thaw are too short to be observed in the coarse-resolution, long-term ^{14}C record, indicating that CO_2 sequestration dominates the long-term temporal trend.

The ^{210}Pb -based aCar for permafrost plateaus at our site was similar to those reported for other nearby permafrost plateaus [Turetsky *et al.*, 2000]. The aCar for the bog features were on the same order though slightly higher than those reported for an Alaskan bog system postburn [Myers-Smith *et al.*, 2007b] and much higher than the average accumulation rate for peatlands overall. Low accumulation rates led those

researchers to suggest that fire increases bog extent and C storage in collapse features. As seen in other studies, drought decreased the C storage potential of the surrounding landscape so temperature and moisture content appear to be the largest drivers of C storage potential in peatlands [Myers-Smith et al., 2007a, 2007b; Schädel et al., 2016].

In Alaska, the functioning of permafrost plateaus as net CO₂ sources or sinks is controlled by ecosystem respiration rates which in turn appear to be controlled by growing season temperatures [Euskirchen et al., 2014], moisture content, and vascular vegetation cover [Myers-Smith et al., 2007a], while gross primary productivity in the plateaus does not appear to vary significantly from year to year [Euskirchen et al., 2014]. Drier conditions on the plateaus lead to lower net CO₂ uptake and lower CH₄ emission, while thawing and collapse lead to wetter conditions. These wetter conditions favor photosynthesis, especially by vascular moat-associated plants such as *Eriophorum* spp., which increases net CO₂ uptake while at the same time contributing to anoxia which favors CH₄ emissions. In highly productive moat areas, primary production outweighs anaerobic decomposition rates and the sites remain net C sinks [Myers-Smith et al., 2007a]. In general, CH₄ emission is highest at thawed wet sites that favor primary production from vascular plants and anoxic subsurface conditions [Myers-Smith et al., 2007a, 2007b; Johnston et al., 2014].

From these cumulative results, we propose the following progression of these ecosystems in response to current warming trends. Prior to the initiation of climate warming in the discontinuous permafrost zone, the peat cycled between permafrost and wetland repeatedly, as described by Zoltai [1993]. Most of the C accumulation occurred during the wetland phases of the landform-consistent with the dominance of Sphagnum-derived organic material in the peat record. During the permafrost plateau phases, the landforms acted as weak net CO₂ sinks, where ecosystem respiration was suppressed by the cold temperatures and inaccessibility of frozen peat organic matter. C sink activity was controlled by the rate of net ecosystem production resulting in slow peat accumulation rates and moderate C storage. With recent climatic warming, ecosystem respiration has increased, resulting in a shift of the peatland plateau into a weaker C sink or even a C source. With continued warming, or a fire that destroys the shading trees, permafrost thaws, the plateau collapses, floods, and ecosystem respiration become suppressed by the resulting anaerobic conditions. Primary productivity of aquatic macrophytes is stimulated by the thaw conditions of the moat environment creating a strong CO₂ sink. Our gas flux and ²¹⁰Pb measurements indicate that the moats act as net C sinks through the accumulation of peat organic matter. However, methanogenesis is stimulated in the anaerobic conditions of the moat leading to the emission of CH₄ from sites that previously had little to no CH₄ flux.

4.3. Radiative C Flux: Net Greenhouse Gas Effect

In general, these thaw features act as net C sinks whether considered over the last few decades or since the end of the mid-Holocene. This is because, over the lifetime of the peat, gross primary productivity has been greater than ecosystem respiration resulting in the accumulation of the peat. We have shown, though, that when these systems thaw, they emit more CH₄ at least on the decadal-scale, postthaw [e.g., Johnston et al., 2014]. Because CH₄ absorbs more infrared radiation on a mol per mol basis than CO₂ it has a higher global warming potential—especially in the short term. Net radiative C flux takes into account both the stronger radiative efficiency (IR absorption efficiency) and the shorter atmospheric lifetime of CH₄ in the atmosphere, relative to CO₂ [Whiting and Chanton, 2001]. Thus, if we are interested in the net effect that thawing permafrost has on climate, we need to consider net radiative C flux at our sites.

Net radiative forcing (RF) results show that the peat has a net warming effect on climate only during the initial thaw cycle (Figure 6). In each subsequent cycle the thaw event pushes the RF temporarily toward positive values, without ever actually achieving net positive forcing (i.e., warming) again, relative to the initial state in the mid-Holocene. The effect of thaw events is minimal in the overall trend of radiative forcing over the lifetime of the peatland. The trend is dominated by weak C uptake during the long plateau stages and stronger C uptake during the wetland stages. The cumulative RF over the lifetime of the peatland differed little between the short-frequency (600 years) and long-frequency (1000 years) simulations. When considered on the scale of a few centuries these peatlands act as net C sinks despite temporary short-term increases in greenhouse gas emissions. Further, the trend in net RF is generally consistent with the ¹⁴C results, suggesting that peat is accumulating at a nearly constant rate regardless of intervening permafrost-thaw cycles.

In the second set of modeling exercises, we projected what would occur if—due to climatic warming—permafrost never reformed and the system remained thawed with differing levels of CH₄ emissions (Figure S2). In each case, projections show that permafrost thaw results in the system trending toward positive forcing, but over time the strength of that trend diminishes until the system trends toward increased negative forcing again. Even in scenarios where CH₄ emissions were allowed to increase up to one half of CO₂ uptake rates on a molar basis (i.e., 2 orders of magnitude higher than current measured values) and net forcing does become temporarily positive, the system nevertheless returns to net negative radiative forcing (i.e., cooling). The amount of time this trend reversal takes, however, does vary according to the ratio between CO₂ uptake and CH₄ emissions. Higher CH₄ emissions increase the magnitude of the trend reversal and prolong the time it takes for the system to return to its original downward trend. In the case where CH₄ emissions are one half CO₂ uptake it takes the system approximately 500 years to return to net cooling.

O'Donnell *et al.* [2012] observed enhanced decomposition following the collapse of thaw features that initially released large amounts of organic C from depth—up to 40% of total C stocks, such a transient rapid loss of C could explain the discrepancies between ²¹⁰Pb and ¹⁴C-based aCar. To investigate the effects of such a response, we ran the radiative forcing model again using our long-frequency permafrost-thaw cycling scenario, this time iteratively solving for the amount of C that would need to be emitted from the moat feature to result in a C inventory that matches the ¹⁴C-based moat inventory. Given that we only observed net C uptake in our flux chamber measurements of moat features at this site, which we could not use our flux measurements to reconcile modeled C inventories with observed ¹⁴C-based inventories. Therefore, we modeled C loss during the moat stages as occurring in a CO₂:CH₄ = 10, a value we have observed at other thaw sites [e.g., Hodgkins *et al.*, 2015]. This scenario created temporary high positive (warming) excursions for the net RF of the peatland upon thawing (Figure 7b). However, after the initial pulse of C from the peatland, as emissions were allowed to relax toward measured flux values for each of the features, the system trended back toward negative RF and when viewed over the lifetime of the peat, despite the high positive RF excursions, the peatland remained a net C sink with a concomitant cooling effect on the atmosphere. It should be noted that flux rates as high as were needed to match ¹⁴C-aCar in this model were never observed using our flux chambers at the site, in spite of the acknowledgment that CO₂ uptake was likely underestimated due to the exclusion of trees from flux chambers. This may reflect a limitation of the chamber measurements and may have occurred because no features were measured soon enough after thaw to capture the rapid pulse of net C emissions. Our assumption that wintertime fluxes could be represented by the January chamber measurements may have biased the winter results toward lower fluxes associated with cold temperatures. Other possible sources of uncertainty from the flux measurements include a springtime flush or the presence of taliks that could stimulate winter losses via localized pipes. Our measurements in May, when snow and ice were still present at the site, could have captured a springtime flush. However, while we did not detect any elevated emissions during the winter that would suggest losses via pipes, the heterogeneous nature of such losses makes it difficult to determine whether and to what extent such losses may have occurred. Further, our model does not account for the rapid loss of C due to fire potentially present at the initiation of each thaw cycle. However, the rates of C loss needed to reconcile the ¹⁴C-based peat accumulation with the model results (i.e., 4.3 kg C m⁻² yr⁻¹ for the first 10 years of each thaw cycle) are even higher than the average C loss from peatlands during a fire event (3.2 kg C m⁻² [Turetsky *et al.*, 2002]).

Because we used the ²¹⁰Pb-based accumulation rates to estimate C sequestration rates in the model, decomposition and loss of C from peat deeper than the ²¹⁰Pb depth would not be accounted for in our ²¹⁰Pb-aCar-derived CO₂ uptake rates. Since we do not know the exact timing of the thaw events at the eight sites relative to our field visits in 2001 and 2002, we do not know the complete flux time series from thaw to permafrost reformation. We do know that on average the most recently thawed sites (moats) are the strongest C sinks, while the midbog sites are near C neutral (Figures 2 and 3) implying that if there was a period of rapid C loss from deeper/older sylvic peat upon thaw (as observed by O'Donnell *et al.* [2012] in Alaska) it had stopped or slowed substantially by the time we measured fluxes in the moats. We also know that when integrated over the last ~100 years using the ²¹⁰Pb-aCar, the bog-moat transitions are also net C sinks implying that these sites have consistently acted as net C sinks for ~100 years before and during bog redevelopment and prior to permafrost reformation. The ²¹⁰Pb cores extend 0.5–1.0 m below the surface. If these sites follow Zoltau's [1993] characterizations of years for subsidence, decades for uplift and centuries for postsubsidence peat

accumulation, it is unlikely that the collapse feature is much more than 100 years old, and despite the possibility of brief initial C losses, there has been persistent C uptake over that time. *O'Donnell et al.* [2012] estimated the period of C loss for collapse-scar bogs in central Alaska as occurring over the first 100 years with very little new peat C formation during the first ~50 years (their Figure 7b). Their young-bog plots had 0.5–4 kg C bog peat, which is 4–30 cm based on their $0.0131 \text{ g C cm}^{-3}$ bulk density (their Tables 1 and 3). So while both sites could be following a thaw-leads-to-C-loss followed-by-C-gain-followed-by-permafrost recovery trajectory, it would appear that the Alberta sites have a shorter period of net C loss (if they have one at all) and more rapid transition to an interval of strong C gain.

Another possible explanation for the discrepancy between ^{210}Pb - and ^{14}C -based accumulation rates is that decomposition could be occurring at depths greater than the oldest ^{210}Pb dateable horizons and/or that accumulation rates have recently increased above mean rates over the lifetime of the peat. Finally, if peat accumulation rates had recently increased, then estimates of C sequestration during previous thaw cycles may be overestimated in our model. Nevertheless, the final modeling exercise shows that even if CO_2 emissions were highly positive for a brief period following thaw and CH_4 emissions were roughly 2 orders of magnitude higher than any measured flux rates, the peatland remains a net C sink, although a weaker one, and still has an overall net cooling effect on climate when considered over the lifetime of the system.

5. Conclusions

Gas flux data and C balance calculations demonstrate that the inundated wetland-like portions of the thaw features (moats) act as CO_2 sinks and CH_4 sources with the net result that most of these sites are net C sinks. Cumulatively, the ^{210}Pb and ^{14}C results suggest that the highest rates of primary production at these sites has occurred within the last few decades as indicated by the subsurface maximum in many of the ^{210}Pb profiles, perhaps stimulated by the increasing warming trend and/or increased N deposition. While flooded thaw features contribute to CH_4 emissions through degradation of both peat and fresh organic matter produced by the enhanced primary productivity at these sites, these sites are also areas of enhanced peat accumulation. The higher peat accumulation rates at the surface (determined by ^{210}Pb dating) relative to the deeper cores (determined from ^{14}C results) demonstrate that while some peat may be degraded with the warmer, wetter conditions, overall peat is being formed at a faster rate than it is getting degraded and the net result is C sequestration.

The implications of the modeling exercises are many. (1) When considered in the long view (millennia) thawing peatlands, despite brief excursions toward net warming, will inevitably have a net cooling effect on climate, unless the system reaches an unforeseen threshold tipping point. For example, if fire frequency and severity increased, causing large episodic losses of peat C, or if heterotrophic respiration rates increased and became less dependent on contemporary primary production [e.g., *Chanton et al.*, 2008; *Wilson et al.*, 2016], or otherwise started consuming more solid peat, the moat habitat could become a net CO_2 source and/or have CH_4 emissions greater than net CO_2 uptake, i.e., degradation of peat stores. In this manner, the system could achieve sustained net positive forcing. (2) The initial increase in radiative forcing following thaw indicates that the system becomes a source of net climate warming in the short term which could have cascading effects on short-lived processes such as vegetation cover or microbial community dynamics that could contribute to the kind of tipping point described above. (3) The length of time it takes the system to return to its previous net cooling capacity following thaw is driven by CO_2 : CH_4 flux ratios, suggesting that the time scale under consideration and CO_2 : CH_4 emissions dynamics are tightly coupled and that both need to be considered equally in determining the response of peatlands to future climate warming.

On balance these peatlands have acted as net C sinks, attenuating climate warming through their uptake of CO_2 , throughout the last several millennia [Zoltai, 1993]. The plateaus may briefly (on the order of years to decades) act as CO_2 sources depending on temperature and ecosystem respiration rates, but when integrated over the lifetime of the peat, these sites have acted as net C sinks via peat accumulation. In greenhouse gas terms, the transition at these features from permafrost (plateau) to wetland (moats) are accompanied by increasing CO_2 uptake that is partially offset by increasing CH_4 emissions (which is a stronger greenhouse gas than CO_2). In the short term (≤ 100 year time scale) the net climatic effect of this transition

is likely to be enhanced warming via increased radiative C emissions, while in the long term (>500 years) the net C deposition at many of the sites appears to result in a negative feedback to climate warming.

Acknowledgments

This work was supported, in part, by the U.S. Department of Energy Office of Biological and Environmental Research under the Genomic Science program (awards DE-SC0004632, DESC0010580, and DESC0016440) and in part by the Office of Biological and Environmental Research, Terrestrial Ecosystem Science Program, under U.S. Department of Energy contract DE-SC0012088. Supporting data are included as three tables in a supporting information file; additional modeling data may be obtained from R.M.W. (e-mail: rmwilson@fsu.edu). The authors declare no competing interests.

References

- Appleby, P. G. (1993), Forward to the lead-210 dating anniversary series, *J. Paleolimnol.*, **9**, 155–160.
- Appleby, P. G., and F. Oldfield (1978), The calculations of lead-210 dates assuming a constant rate of supply of unsupported 210Pb to the sediment, *Catena*, **5**, 1–8.
- Appleby, P. G., and F. Oldfield (1983), The assessment of 210Pb data from sites with varying sediment accumulation rates, *Hydrobiologia*, **103**, 29–35.
- Backstrand, K., P. M. Crill, M. Jackowicz-Korczynski, M. Mastepanov, T. R. Christensen, and D. Bastviken (2010), Annual carbon gas budget for a subarctic peatland, Northern Sweden, *Biogeosciences*, **7**, 95–108.
- Beilman, D. W., D. H. Vitt, and L. A. Halsey (2001), Localized permafrost peatlands in western Canada: Definition, distributions, and degradation, *Arct. Antarct. Alp. Res.*, **33**, 70–77.
- Bellisario, L. M., J. L. Bubier, T. R. Moore, and J. P. Chanton (1999), Controls on CH₄ emissions from a northern peatland, *Global Biogeochem. Cycles*, **13**, 81–91, doi:10.1029/1998GB900021.
- Blanc-Betes, E., J. M. Welker, N. C. Sturchio, J. P. Chanton, and M. A. Gonzalez-Meler (2016), Increases in winter precipitation and snow accumulation transform Arctic tundra from a sink to a source of methane, *Global Change Biol.*, doi:10.1111/gcb.13242.
- Camill, P. (1999), Patterns of boreal permafrost peatland vegetation across environmental gradients sensitive to climate warming, *Can. J. Bot.*, **77**(5), 721–733.
- Camill, P., and J. S. Clark (1998), Climate change disequilibrium of boreal permafrost peatlands caused by local processes, *Am. Natural.*, **151**(3), 207–222.
- Chanton, J. P., and G. Whiting (1995), Trace gas exchange in freshwater and coastal marine environments: Ebullition and transport by plants, in *Biogenic Trace Gases: Measuring Emissions From Soil and Water*, pp. 98–125, Blackwell Sci., London, England.
- Chanton, J. P., G. J. Whiting, W. J. Showers, and P. M. Crill (1992a), Methane flux from *Peltandra virginica*: Stable isotope tracing and chamber effects, *Global Biogeochem. Cycles*, **6**, 15–31, doi:10.1029/91GB02969.
- Chanton, J. P., C. S. Martens, C. A. Kelley, P. M. Crill, and W. J. Showers (1992b), Methane transport mechanisms and isotopic fractionation in emergent macrophytes of an Alaskan Tundra lake, *J. Geophys. Res.*, **97**, 16,681–16,688, doi:10.1029/90JD01542.
- Chanton, J. P., P. H. Glaser, L. S. Chasar, D. J. Burdige, M. E. Hines, D. I. Siegel, L. B. Tremblay, and W. T. Cooper (2008), Radiocarbon evidence for the importance of surface vegetation on fermentation and methanogenesis in contrasting types of boreal peatlands, *Global Biogeochem. Cycles*, **22**, GB4022, doi:10.1029/2008GB003274.
- Christensen, T., et al. (2013), *The Arctic Terrestrial Biodiversity Monitoring Plan, CAFF Monitoring Ser. Rep. No. 7*, CAFF International Secretariat, Akureyri, Iceland.
- Corbett, J. E., D. J. Burdige, M. M. Tfaily, A. R. Dial, W. T. Cooper, P. H. Glaser, and J. P. Chanton (2013), Surface production fuels deep heterotrophic respiration in northern peatlands, *Global Biogeochem. Cycles*, **27**, 1163–1174, doi:10.1002/2013GB004677.
- Eisenhauer, N., S. Cesarz, R. Koller, K. Worm, and P. B. Reich (2012), Global change belowground: Impacts of elevated CO₂ nitrogen, and summer drought on soil food webs and biodiversity, *Global Change Biol.*, **18**, 435–447.
- Elberling, B., A. Michelsen, C. Schadel, E. A. G. Schuur, H. H. Christiansen, L. Berg, M. P. Tamstorf, and C. Sigsgaard (2013), Long-term CO₂ production following permafrost thaw, *Nat. Clim. Change*, **3**, 890–894.
- Eliasson, P. E., R. E. McMurtrie, D. A. Pepper, M. Strömberg, S. Linder, and G. I. Ågren (2005), The response of heterotrophic CO₂ flux to soil warming, *Global Change Biol.*, **11**, 167–181, doi:10.1111/j.1365-2486.2004.00878.x.
- Euskirchen, E. S., C. W. Edgar, M. R. Turetsky, M. P. Waldrop, and J. W. Harden (2014), Differential response of carbon fluxes to climate in three peatland ecosystems that vary in the presence and stability of permafrost, *J. Geophys. Res. Biogeosci.*, **119**, 1576–1595, doi:10.1002/2014JG002683.
- Frey, K. E., and J. W. McClelland (2008), Impacts of permafrost degradation on arctic river biogeochemistry, *Hydrol. Process.*, **23**, 169–182.
- Frolking, S., N. Roulet, and J. Fuglestad (2006), How northern peatlands influence the Earth's radiative budget: Sustained methane emission versus sustained carbon sequestration, *J. Geophys. Res.*, **111**, G01008, doi:10.1029/2005JG000091.
- Frolking, S., J. Talbot, and Z. M. Subin (2014), Exploring the relationship between net carbon balance and apparent carbon accumulation rate at century to millennial time scales, *Holocene*, **24**, 1021–1027.
- Goulden, M. L., B. C. Daube, S.-M. Fan, D. J. Sutton, A. Bazzaz, J. W. Munger, and S. C. Wofsy (1997), Physiological responses of a black spruce forest to weather, *J. Geophys. Res.*, **102**, 28,987–28,996, doi:10.1029/97JD01111.
- Halsey, L. A., D. H. Vitt, and S. C. Zoltai (1995), Disequilibrium response of permafrost in boreal continental western Canada to climate change, *Clim. Change*, **30**, 57–73.
- Hicks Pries, C. E., E. A. G. Schuur, and K. G. Crummer (2011), Holocene carbon stocks and carbon accumulation rates altered in soils undergoing permafrost thaw, *Ecosystems*, **15**, 162–173.
- Hicks Pries, C. E., E. A. G. Schuur, and K. G. Crummer (2013), Thawing permafrost increases old soil and autotrophic respiration in tundra: Partitioning ecosystem respiration using $\delta^{13}\text{C}$ and $\Delta^{14}\text{C}$, *Global Change Biol.*, **19**, 649–661.
- Hodgkins, S. B., J. P. Chanton, C. C. Langford, C. K. McCalley, S. R. Saleska, V. I. Rich, P. M. Crill, and W. T. Cooper (2015), Soil incubations reproduce field methane dynamics in a subarctic wetland, *Biogeochemistry*, **126**, 241–249.
- Hogg, E. H., V. J. Lieffers, and R. W. Wein (1992), Potential carbon losses from peat profiles: Effects of temperature, drought cycles and fire, *Ecol. Appl.*, **2**(3), 298–306.
- Hugelius, G., et al. (2014), Estimated stocks of circumpolar permafrost carbon with quantified uncertainty ranges and identified data gaps, *Biogeosciences*, **11**, 6573–6593.
- Johnston, C. E., S. A. Ewing, J. W. Harden, R. K. Varner, K. P. Wickland, J. C. Koch, C. C. Fuller, K. Manies, and M. T. Jorgenson (2014), Effect of permafrost thaw on CO₂ and CH₄ exchange in a western Alaska peatland chronosequence, *Environ. Res. Lett.*, **9**, 085004, doi:10.1088/1748-9326/9/8/085004.
- Jones, M. C., R. K. Booth, Z. Yu, and P. Ferry (2013), A 2200-year record of permafrost dynamics and carbon cycling in a collapse-scar bog, interior Alaska, *Ecosystems*, **16**, 1–29.
- Jones, M. C., J. Harden, J. O'Donnell, K. Manies, T. Jorgenson, C. Treat, and S. Ewing (2016), Rapid carbon loss and slow recovery following permafrost thaw in boreal peatlands, *Global Change Biol.*, doi:10.1111/gcb.13403.

- Joos, F., et al. (2013), Carbon dioxide and climate impulse response functions for the computation of greenhouse gas metrics: A multi-model analysis, *Atmos. Chem. Phys.*, *13*, 2793–2825.
- Kawahigashi, M., K. Kaiser, K. Kalbitz, A. Rodionov, and G. Guggenberger (2004), Dissolved organic matter in small streams along a gradient from discontinuous to continuous permafrost, *Global Change Biol.*, *10*, 1576–1586.
- Melillo, J. M., P. A. Steudler, J. D. Aber, K. Newkirk, H. Lux, F. P. Bowles, C. Catricala, A. Magill, T. Ahrens, and S. Morriseau (2002), Soil warming and carbon-cycle feedbacks to the climate system, *Science*, *298*, 2173–2176.
- Myers-Smith, I. H., J. W. Harden, M. Wilmking, C. C. Fuller, A. D. McQuire, and F. S. Chapin III (2007a), Wetland succession in a permafrost collapse: Interactions between fire and thermokarst, *Biogeosci. Discuss.*, *4*, 4507–4538.
- Myers-Smith, I. H., A. D. McQuire, J. W. Harden, and F. R. Chapin III (2007b), Influence of disturbance on carbon exchange in a permafrost collapse and adjacent burned forest, *J. Geophys. Res.*, *112*, G04017, doi:10.1029/2007/JG000423.
- Natali, S. M., E. A. G. Schuur, and R. L. Rubin (2012), Increased plant productivity in Alaskan tundra as a result of experimental warming of soil and permafrost, *J. Ecol.*, *100*, 488–498.
- Natali, S. M., et al. (2015), Permafrost thaw and soil moisture driving CO₂ and methane release from upland tundra, *J. Geophys. Res. Biogeosci.*, *120*, 525–537, doi:10.1002/2014JG002872.
- Neubauer, S. C., and J. P. Megonigal (2015), Moving beyond global warming potentials to quantify the climatic role of ecosystems, *Ecosystems*, *18*, 1000–1013.
- O'Donnell, J. A., J. W. Harden, A. D. McQuire, M. Z. Kanevskiy, M. T. Jorgenson, and X. Xu (2011), The effect of fire and permafrost interactions on soil carbon accumulation in an upland black spruce ecosystem of interior Alaska: Implications for post-thaw carbon loss, *Global Change Biol.*, *17*, 1461–1474, doi:10.1111/j.1365-2486.2010.02358.x.
- O'Donnell, J. A., M. T. Jorgenson, J. W. Harden, A. D. McQuire, M. Z. Kanevskiy, and K. P. Wickland (2012), The effects of permafrost thaw on soil hydrologic, thermal, and carbon dynamics in an Alaskan peatland, *Ecosystems*, *15*, 213–229.
- Oechel, W. C., S. J. Hastings, G. Vourlitis, M. Jenkins, G. Reichers, and N. Grulke (1993), Recent change of Arctic tundra ecosystems from a net carbon dioxide sink to a source, *Nature*, *361*, 520–523.
- Prater, J., J. P. Chanton, and G. Whiting (2007), Variation in methane production pathways associated with permafrost decomposition in collapse scar bogs of Alberta, Canada, *Global Biogeochem. Cycles*, *21*, GB4004, doi:10.1029/2006GB002866.
- Robinson, S. D., and T. R. Moore (2000), The influence of permafrost and fire upon carbon accumulation in high boreal peatlands, Northwest Territories, Canada, *Arct. Antarct. Alp. Res.*, *32*, 155–166.
- Sadler, P. M. (1981), Sediment accumulation rates and the completeness of stratigraphic sections, *J. Geol.*, *89*(5), 569–584.
- Schädel, C., et al. (2016), Potential carbon emissions dominated by carbon dioxide from thawed permafrost soils, *Nat. Clim. Change*, *6*, 950–953, doi:10.1038/NCLIMATE3054.
- Schuur, E. A. G., et al. (2008), Vulnerability of permafrost carbon to climate change: Implications for the global carbon cycle, *BioScience*, *58*(8), 701–714.
- Schuur, E. A. G., et al. (2015), Climate change and the permafrost carbon feedback, *Nature*, *520*, 171–180.
- Spencer, R. G., P. J. Mann, T. Dittmar, T. I. Eglinton, C. McIntyre, R. M. Holmes, N. Zimov, and A. Stubbins (2015), Detecting the signature of permafrost thaw in Arctic rivers, *Geophys. Res. Lett.*, *42*, 2830–2835, doi:10.1002/2015GL063498.
- Tarnocai, C., J. G. Canadell, E. A. G. Schuur, P. Kuhry, G. Mazhitova, and S. Zimov (2009), Soil organic carbon pools in the northern circumpolar permafrost region, *Global Biogeochem. Cycles*, *23*, GB2023, doi:10.1029/2008GB003327.
- Tfaily, M. M., R. Hamdan, J. E. Corbett, J. P. Chanton, P. H. Glaser, and W. T. Cooper (2013), Investigating dissolved organic matter decomposition in northern peatlands using complimentary analytical techniques, *Geochim. Cosmochim. Acta*, *112*, 116–129.
- Tfaily, M. M., W. T. Cooper, J. E. Kostka, P. R. Chanton, C. W. Schadt, P. J. Hanson, C. M. Iversen, and J. P. Chanton (2014), Organic matter transformation in the peat column at Marcell Experimental Forest: Humification and vertical stratification, *J. Geophys. Res. Biogeosci.*, *119*, 661–675, doi:10.1002/2013JG002492.
- Treat, C. C., W. M. Wollheim, R. K. Varner, A. S. Grandy, J. Talbot, and S. Frohling (2014), Temperature and peat type control CO₂ and CH₄ production in Alaskan permafrost peats, *Global Change Biol.*, *23*, GB2023, doi:10.1111/gcb.12572.
- Turetsky, M. R., R. K. Wieder, C. J. Williams, and D. H. Vitt (2000), Organic matter accumulation, peat chemistry, and permafrost melting in peatlands of boreal Alberta, *Ecoscience*, *7*(3), 379–392.
- Turetsky, M. R., R. K. Wieder, L. Halsey and D. H. Vitt (2002), Current disturbance and the diminishing peatland carbon sink. *Geophys. Res. Lett.* *29*(11), 1526, doi:10.1029/2001GL014000.
- Turetsky, M. R., S. W. Manning, and R. K. Wieder (2004), Dating recent peat deposits, *Wetlands*, *24*(2), 324–356.
- Turetsky, M. R., R. K. Wieder, D. H. Vitt, R. J. Evans, and K. D. Scott (2007), The disappearance of relict permafrost in boreal north America: Effects on peatland carbon storage and fluxes, *Global Change Biol.*, *13*, 1922–1934.
- Vitt, D. H., Y. Li, and R. J. Belland (1995), Patterns of Bryophyte diversity in peatlands of continental western Canada, *Bryologist*, *98*(2), 218–227.
- Vitt, D. H., L. A. Halsey, I. E. Bauer, and C. Campbell (2000a), Spatial and temporal trends in carbon storage of peatlands of continental western Canada through the Holocene, *Can. J. Earth Sci.*, *37*, 683–693.
- Vitt, D. H., L. A. Halsey, and S. C. Zoltai (2000b), the changing landscape of Canada's western boreal forest: The current dynamics of permafrost, *Can. J. For. Res.*, *30*(2), 283–287.
- Whiting, G., and J. P. Chanton (1993), Primary production control of methane emission from wetlands, *Nature*, *26*, 364–365.
- Whiting, G. J., and J. P. Chanton (2001), Greenhouse carbon balance of wetlands: Methane emission versus carbon sequestration, *Tellus*, *53B*, 521–528.
- Wilson, R. M., et al. (2016), Stability of peatland carbon to rising temperatures, *Nat. Commun.*, *7*, 13723, doi:10.1088/ncomms13723.
- Zimov, S. A., S. P. Davydov, G. M. Zimova, A. I. Davydova, E. A. G. Schuur, K. Dutta, and F. S. Chapin III (2006), Permafrost carbon: Stock and decomposability of a globally significant carbon pool, *Geophys. Res. Lett.*, *33*, L20502, doi:10.1029/2006GL027484.
- Zoltai, S. C. (1993), Cyclic development of permafrost in the peatlands of northwestern Alberta Canada, *Arct. Alp. Res.*, *25*(3), 240–246.
- Zoltai, S. C., L. A. Morrissey, G. P. Livingston, and W. J. de Groot (1998), Effects of fires on carbon cycling in North American boreal peatlands, *Environ. Rev.*, *6*, 13–24.